1,2,3,5-Dithiadiazolium Cations and 1,2,3,5-Dithiadiazolyl Radicals: An ab Initio Computational, Ultraviolet Photoelectron Spectroscopic, and Crystallographic Study of a Cation/Radical Pair

A. Wallace Cordes,[1a] John D. Goddard,*[1b] Richard T. Oakley,[1b] and Nicholas P. C. Westwood[1b]

Contribution from the Department of Chemistry and Biochemistry, University of Arkansas, Fayetteville, Arkansas 72701, and the Guelph Waterloo Centre for Graduate Work in Chemistry, Guelph Campus, Department of Chemistry and Biochemistry, University of Guelph, Guelph, Ontario, N1G 2W1, Canada. *Received November 28, 1988*

Abstract: The ground-state molecular structures of the 4-(dimethylamino)-1,2,3,5-dithiadiazolium cation and the corresponding dithiadiazolyl radical have been determined by crystallographic studies on the SbF_6^- salt of the cation and the weakly associated dimer of the radical. Complementary ab initio SCF calculations with RHF, UHF, and ROHF wave functions and 3-21G* and 6-31G* basis sets for the structures of both the unknown 4-amino and the experimentally studied 4-dimethylamino radical and cation ground states are in excellent agreement with experiment, where known. The ground and excited states of the 4-dimethylamino cation have also been studied by electronic spectroscopy and by ultraviolet photoelectron measurements on the cation and radical, respectively. The geometries, energies, and electronic structures of the first three cationic states, $^1A_1$, $^3B_2$, and $^1B_2$, of both the 4-amino and 4-dimethylamino species are evaluated in light of the experimental results and ab initio calculations that include electron correlation via perturbation theory.

The generation, molecular, and electronic structures and spectroscopic properties of 1,2,3,5-dithiadiazolium cations (**1a**) and the corresponding dithiadiazolyl radicals **1b** are subjects of current interest.[2] Radicals with a variety of R groups have been

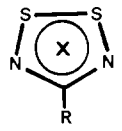

1a (X = +) **1b** (X = •)

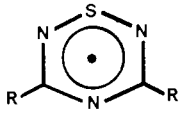

2

studied by ESR spectroscopy,[3] and the structures of radical dimers of the 4-phenyl[4] and 4-CF_3[3a] derivatives have been determined crystallographically. The structure of the 4-CF_3 species has also been studied in the gas phase.[3a] More recently the electronic structures of several dithiadiazolyl **1b** and thiatriazinyl **2** radicals (R = Ph, Cl, CF_3) were probed by ultraviolet photoelectron spectroscopy (UPS).[5] Using semiempirical molecular orbital (MNDO) calculations and systematic trends in radical ionization potentials (IPs), preliminary assignments of the ground and low-lying excited cationic states arising from photoionization of the radicals were put forward.

In the present paper we extend and enhance the earlier work with a combined structural (X-ray diffraction), ultraviolet photoelectron, and ab initio molecular orbital analysis of a single cation/radical pair, namely, the 4-dimethylamino derivatives **1a** and **1b** (R = NMe_2). Collectively and in combination with calculations on the 4-amino derivative, the results allow a unique opportunity for establishing very precise information on the ground states of the cation ($^1A_1$) and radical ($^2A_2$). In addition, the molecular structures of the first excited triplet ($^3B_2$) and singlet ($^1B_2$) cationic states arising from excitation of an electron from the nitrogen-based "lone-pair" highest occupied molecular orbital (HOMO, b_1) to the lowest unoccupied molecular orbital (LUMO,

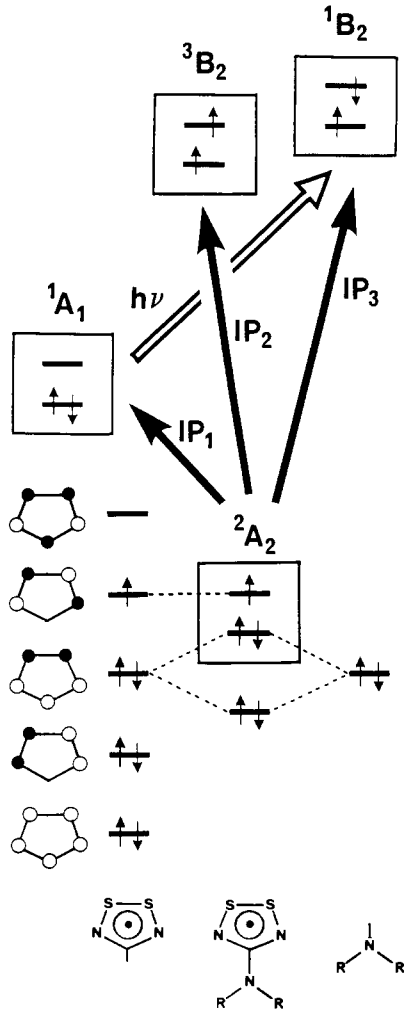

Figure 1. π molecular orbital manifold of the $^2A_2$ dithiadiazolyl radical **1b** (R = NR_2) and the lowest lying cationic states accessible by ionization and excitation.

(1) (a) University of Arkansas. (b) University of Guelph.
(2) Oakley, R. T. *Prog. Inorg. Chem.* **1988**, *36*, 299.
(3) (a) Höfs, H.-U.; Bats, J. W.; Gleiter, R.; Hartmann, G.; Mews, R.; Eckert-Maksič, M.; Oberhammer, H.; Sheldrick, G. M. *Chem. Ber.* **1985**, *118*, 3781. (b) Markovskii, L. N.; Polumbrik, P. M.; Talanov, V. S.; Shermolovich, Yu. G. *Tetrahedron Lett.* **1982**, *23*, 761. (c) Müller, T. Dissertation, University Frankfurt, 1979. (d) Fairhurst, S. A.; Johnson, K. M.; Sutcliffe, L. H.; Preston, K. F.; Banister, A. J.; Hauptmann, Z. V.; Passmore, J. *J. Chem. Soc., Dalton Trans.* **1986**, 1465.
(4) Vegas, A.; Pérez-Salazar, A.; Banister, A. J.; Hey, R. G. *J. Chem. Soc., Dalton Trans.* **1980**, 1812.
(5) Boeré, R. T.; Oakley, R. T.; Reed, R. W.; Westwood, N. P. C. *J. Am. Chem. Soc.* **1989**, *111*, 1180.

0002-7863/89/1511-6147$01.50/0

a_2; see Figure 1) can also be probed by computation. The associated adiabatic and vertical energy differences between the neutral radical and the cations calculated at the SCF and correlated levels provide accuracies beyond simple Koopmans' theorem arguments and verify the assignment of the low-energy region of the photoelectron spectrum, including the observed splitting between the triplet and singlet excited states.

Experimental and Computational Methods

Preparation of 1a (R = NMe_2). The 4-(dimethylamino)-1,2,3,5-dithiadiazolium cation (**1a**, R = NMe_2) was prepared, as its chloride salt, by the reaction of *N,N*-dimethylguanidinium hydrochloride (Aldrich) with excess sulfur dichloride (Aldrich) in acetonitrile (distilled from P_2O_5). A mixture of $Me_2NC(NH)NH_2$·HCl (2.00 g, 16.2 mmol) and excess SCl_2 (4 mL) was heated at reflux for 12 h (shorter reaction times lead to much poorer yields) in 50 mL of CH_3CN. The resulting deep purple solution was cooled to −20 °C for several hours and then filtered to give 2.1 g of an almost black crystalline mass. This solid was recrystallized from acetonitrile to afford deep purple crystals of $[(Me_2N)CN_2S_2]^+Cl^-$ (1.6 g, 8.7 mmol, 54% yield); mp 179–82 °C, λ_{max} (in CH_3CN) 532 ($\epsilon = 3 \times 10^2$ M^{-1} cm^{-1}) and 398 (2×10^2 M^{-1} cm^{-1}) nm. Anal. Calcd for $C_3H_6N_3S_2Cl$: C, 19.62, H 3.29, N, 22.88, Cl, 19.30. Found: C, 19.81; H, 3.45; N, 22.53; Cl, 19.51. IR (Nujol mull) 1570 (s), 1401 (m), 1296 (w), 1244 (m), 1178 (m), 1179 (w), 1131 (m), 1081 (m), 1062 (m), 930 (s), 889 (s), 706 (s), 570 (s), 533 (w), 457 (m) cm^{-1}. Metathesis of this chloride salt of **1a** (R = NMe_2) with nitrosyl hexafluoroantimonate (Alfa) in benzonitrile afforded, upon careful evaporation of the solvent, the corresponding SbF_6^- salt as deep-purple crystalline plates. These latter crystals were used for X-ray work.

Preparation of 1b (R = NMe_2). Reduction of $[(Me_2N)CN_2S_2]^+Cl^-$ (0.60 g, 3.3 mmol) with zinc powder (0.21 g, 3.3 mmol) in 10 mL of liquid SO_2 produced the radical **1b** (R = NMe_2), which was isolated as its dimer by sublimation at 30 °C/0.1 Torr onto a water-cooled finger (yield 0.19 g, 1.3 mmol, 39%). The dimer forms deep-purple (metallic green to reflected light) crystals, dec >90 °C. Anal. Calcd for $C_6H_{12}N_6S_4$: C, 24.31; H, 4.08; N, 28.35. Found: C, 23.85; H, 4.42; N, 27.70. IR (Nujol mull) 1533 (s), 1401 (s), 1312 (m), 1251 (s), 1241 (s), 1070 (w), 1058 (w), 1016 (w), 892 (s), 864 (m), 801 (m), 779 (s), 666 (w), 542 (m), 534 (m), 449 (w) cm^{-1}. The ESR spectrum of **1b** (R = NMe_2), recorded at 22 °C in methylene chloride solution with a Varian E-109 spectrometer exhibits a five-line pattern ($g = 2.0102$, $a_N = 0.50$ mT) typical of the 1,2,3,5-dithiadiazolyl ring system.[3]

X-ray Structure Determinations. All X-ray data (Supplementary Material (see the paragraph at the end of the article)) for $[(Me_2N)CN_2S_2]^+[SbF_6]^-$ and $[(Me_2N)CN_2S_2]_2$ were collected on an ENRAF-Nonius CAD-4 at 293 K with graphite-monochromated Mo Kα (λ = 0.71073 Å) radiation. Crystals were mounted in Lindemann capillaries and sealed with epoxy. In the case of the cation four full data sets were collected, and all were disordered.[6] The results provided here come from the crystal that gave the best refinement. Both structures were solved by using MULTAN and refined by full-matrix least-squares methods which minimized $\sum w(\Delta F)^2$. In the radical dimer structure H atoms were refined isotropically, all other atoms anisotropically ($R = 0.030$, $R_w = 0.040$).

In the cation structure the asymmetric unit of the cell contains two half-cations and two half-anions; crystallographic mirror planes bisect the ions, with the plane of the cations perpendicular to the mirror plane. The SbF_6^- anion of Sb(2) is disordered; 85% of the ion is in the orientation described by F(5–8), 15% in the position related by rotation and involving also F(9) and F(10). In addition Sb(3–6) atoms with occupation factors 0.02 represent a disorder of anions on the mirror plane and along the line between the major component anions. No F atoms were located for these latter Sb atoms. The largest peaks and troughs on the final difference map were within 0.6 Å of these minor-component Sb atoms and indicate either a large anisotropic motion of these atoms or a multipositional aspect of the disorder. The orientations of the methyl groups were determined from a difference map, and the H atoms then constrained to idealized positions with $B = 1.2B$ of the attached carbon. The relatively high R factor ($R = 0.065$, $R_w = 0.108$) and the large estimated standard deviations for the derived distances and angles are attributed to refinement problems related to the modeling of the disorder of the crystal. The high thermal parameters also reflect the "softness" of the packing of the ions.

Atomic scattering factors and anomalous dispersion corrections were taken from the International Tables for X-ray Crystallography.[7] All programs used were those provided by the Enraf-Nonius structure determination package.

Ultraviolet Photoelectron Spectroscopy. The He(I) photoelectron spectrum of **1b** (R = NMe_2) was obtained from the vapor above the radical dimer. Spectra were recorded on an instrument specifically designed to study labile species[8] and calibrated with Ar and CH_3I. Resolution was 45 meV during data acquisition.

Computational Models and Methods. Quite reliable structures have been obtained for a vast number of molecules and radicals from ab initio SCF calculations with split valence, or larger, basis sets.[9] Although less numerous, examples of conventional ab initio Hartree–Fock SCF and CI calculations on sulfur–nitrogen heterocycles are also available.[10]

In the present study we have performed calculations on two dithiadiazolium cations (**1a**, with R = NMe_2 and NH_2) and two dithiadiazolyl radicals (**1b**, also with R = NMe_2 and NH_2). Most of the ab initio computations were performed with the CRAY COS version of GAUSSIAN86, release C.[11] The open-shell singlet restricted Hartree–Fock calculations were carried out with an IBM version of a revised and extended GAMESS package.[12] For both radicals all geometric parameters for the $^2A_2$ ground state were optimized within a C_{2v} symmetry constraint (with, for R = NMe_2, four endo hydrogens) at the 3-21G*[13] SCF level by using energy gradient methods. The lowest three states ($^1A_1$, $^{3,1}B_2$) of both cations were also optimized within C_{2v} symmetry at the 3-21G* level. For the radicals and the triplet state of the cations the calculations were performed using both unrestricted Hartree–Fock (UHF)[14] and restricted open-shell Hartree–Fock (ROHF)[15] SCF procedures. In addition and in order to assess the effects of basis set extension on structure, the geometries of the ground states of **1a** and **1b** (R = NH_2) were further refined at the 6-31G*[16] level. Calculations on the **1a**/**b** (R = NMe_2) pair

Table I. Mean Endocyclic Bond Lengths (Å) and Angles (deg) in Dithiadiazolium Cations **1a** and Dithiadiazolyl Radicals **1b**

1a

R	NMe_2	Cl	CF_3[a]
S–S	2.022 (7)	1.996 (2)	1.989 (3)
S–N	1.586 (9)	1.573 (5)	1.589 (6)
N–C	1.353 (10)	1.321 (8)	1.323 (10)
S–S–N	95.4 (4)	95.4 (2)	94.4 (2)
S–N–C	115.6 (9)	114.4 (4)	113.1 (4)
N–C–N	118.5 (10)	120.3 (5)	118.6 (6)
ref	this work	19	3a

1b

R	NMe_2[b]	CF_3[b]	CF_3[a]	CF_3[c]	Ph[b]
S–S	2.080 (1)	2.087 (2)	2.086 (2)	2.113 (6)	2.089
S–N	1.627 (2)	1.630 (5)	1.640 (5)	1.623 (3)	1.63
N–C	1.348 (2)	1.318 (7)	1.328 (8)	1.318 (6)	1.33
S–S–N	94.99 (6)	94.6 (2)	94.8 (3)	93.95 (5)	94.1
S–N–S	113.8 (1)	112.4 (4)	112.9 (5)	113.9 (6)	116
N–C–N	122.4 (2)	126.1 (5)	124.9 (5)	124.4 (11)	121
ref	this work	3a	3a	3a	4

[a] From mixed-valence cation/radical dimer salt. [b] From radical dimer. [c] From gas-phase radical.

(6) Three data sets were also collected on crystals of the PF_6^- salt. The disorder problem in this derivative was even more chronic. Apparently the small planar cation with large spherical anions leads to disorder very readily.

(7) Cromer, D. T.; Waber, J. T. *International Tables for X-ray Crystallography*; Kynoch Press: Birmingham, England, 1974; Vol IV, Tables 2.2B and 2.3.1.
(8) Sammynaiken, R. M.Sc. Thesis, University of Guelph, 1988.
(9) Hehre, W. J.; Radom, L.; Schleyer, P. v. R.; Pople, J. A. *Ab Initio Molecular Orbital Theory*; Wiley: New York, 1986.
(10) (a) Nguyen, M.-T.; Ha, T.-K. *J. Mol. Struct. (THEOCHEM)* **1983**, *105*, 129. (b) Palmer, M. H.; Guest, M. F. *Chem. Phys.* **1986**, *110*, 187. (c) Lau, W. M.; Westwood, N. P. C.; Palmer, M. H. *J. Am. Chem. Soc.* **1986**, *108*, 3229. (d) Hoffmeyer, R. E.; Chan, W.-T., Goddard, J. D.; Oakley, R. T. *Can. J. Chem.* **1988**, *66*, 2279.
(11) Frisch, M.; Binkley, J. S.; Schlegel, H. B.; Raghavachari, K.; Martin, R.; Stewart, J. J. P.; DeFrees, D.; Seeger, R.; Whiteside, R.; Fox, D. Fluder, E.; Pople, J. A. GAUSSIAN86, Release C. Department of Chemistry, Carnegie-Mellon University, Pittsburgh, PA, 1986.
(12) Dupuis, M.; Spangler, D.; Wendolowski, J. J. *NRCC Program QG01*, 1980, modified by M. Schmidt and S. Elbert.
(13) (a) Binkley, J. S.; Pople, J. A.; Hehre, W. J. *J. Am. Chem. Soc.* **1980**, *102*, 939. (b) Gordon, M. S.; Binkley, J. S.; Pople, J. A.; Pietro, W. J.; Hehre, W. J. *J. Am. Chem. Soc.* **1982**, *104*, 2797.
(14) Pople, J. A.; Nesbet, R. K. *J. Chem. Phys.* **1954**, *22*, 571.
(15) McWeeny, R.; Diercksen, G. H. F. *J. Chem. Phys.* **1968**, *49*, 4852.
(16) (a) Hehre, W. J.; Ditchfield, R.; Pople, J. A. *J. Chem. Phys.* **1972**, *56*, 2257. (b) Francl, M. M.; Pietro, W. J.; Binkley, J. S.; Gordon, M. S.; DeFrees, D. J.; Pople, J. A. *J. Chem. Phys.* **1982**, *77*, 3654. (c) Hariharan, P. C.; Pople, J. A. *Theor. Chim. Acta* **1973**, *28*, 213.

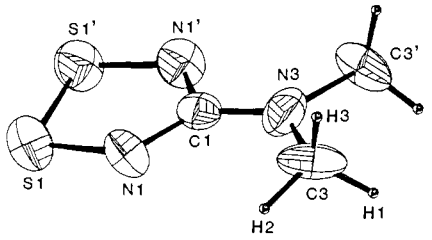

Figure 2. ORTEP drawing (30% probability ellipsoids) of one of the two independent cations in the $[(Me_2N)CN_2S_2]^+[SbF_6]^-$ structure, showing the atom numbering scheme. The connectivity in the other cation is S2–N2–C2–N4–C4.

at this level used the geometries obtained at the 3-21G* level, viz., 6-31G*//3-21G*. The energy differences (ΔSCF) corresponding to ionization potentials IP_1, IP_2, and IP_3 or the excitation energy $h\nu$ (see Figure 1) were refined by means of Møller–Plesset (MP) perturbation theory[17] to as high as partial fourth order ((U)MP4SDQ).[18] The inclusion of electron correlation energy by such MP calculations is critical to the comparison of species with differing numbers of unpaired electrons, e.g., the $^1A_1$ ground-state cations vs $^3B_2$ excited-state cations.

The 3-21G* and 6-31G* calculations on the **1a**/**1b** (R = NH_2) species involved 78 MO/132 primitive Gaussians ("AO") and 102 MO/224 AO functions, respectively. For the **1a**/**1b** (R = NMe_2) pair the basis sets included 104 MO/174 AO (3-21G*) and 140 MO/296 AO (6-31G*).

Results and Discussion

X-ray Crystal Structures. Experimental data (see the supplementary material for full details) on the geometries of **1a** and **1b** (R = NMe_2) were obtained through single-crystal X-ray diffraction studies on the SbF_6^- salt of the cation **1a** and the radical dimer of **1b** (R = NMe_2). A summary of the mean endocyclic structural parameters of both species is provided in Table I, along with the corresponding data for related cations and radicals.

Although a disorder problem (see Experimental and Computational Methods section) in the positions of the anions of the salt structure limited the final *R* value to 6.5%, the absence of any unusually close anion–cation contacts, coupled with the close correspondence between the mean structural parameters of the two independent cations determined here and other reported **1a** structures (R = Cl, CF_3),[3a,19] substantiates the correlation of the cation crystallographic data with the computed isolated molecule to be discussed later. An ORTEP drawing of one of the cations is shown in Figure 2.

The structure of the radical dimer $[(Me_2N)CN_2S_2]_2$ (Figure 3) is of interest for several reasons. The mode of dimerization in particular provides a comparison to that observed in other dithiadiazolyl dimers, for which two modes of association are known. Early work on $[PhCN_2S_2]_2$ revealed the cofacial arrangement **3**,[4] while more recent work on the $[(CF_3)CN_2S_2]_2$

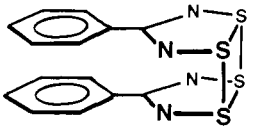

3

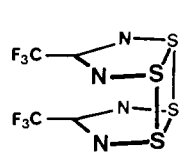

5

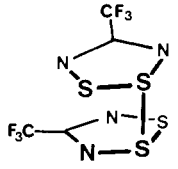

4

derivatives has shown that another conformation, e.g., **4**, is also possible.[3a] The energetic differences between these two possible

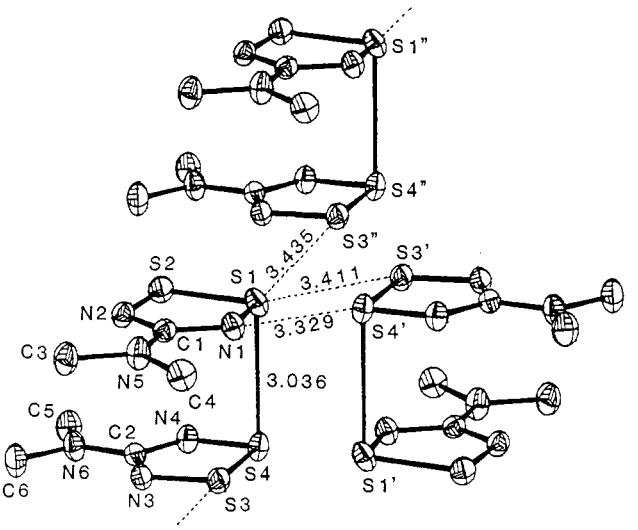

Figure 3. ORTEP drawing (30% probability ellipsoids) of the $[(Me_2N)CN_2S_2]_2$ structure, showing the atom numbering scheme and inter-ring contacts (in angstroms).

geometries are certainly small (MNDO estimates are near 5 kJ/mol);[3a] indeed, the choice between the two is probably controlled more by lattice effects than interannular interactions. This latter point is supported by the fact that in the mixed radical/salt $[(CF_3)CN_2S_2]_3Cl$ the radical dimer adopts a cofacial alignment **5** (analogous to **3**).[3a]

The crystal structure of $[(Me_2N)CN_2S_2]_2$ reveals a dimerization geometry similar to that found for $[(CF_3)CN_2S_2]_2$, i.e., the two five-membered rings are rotated with respect to one another so that there is only one interannular S---S contact of length 3.036 (1) Å. As shown in Figure 3, the dimers are located in pairs about a crystallographic center of symmetry, with short interannular N1---S4′ (3.329 Å) and S1---S3′ (3.411 Å) contacts. Within each pair the S1–S2–N2–C1–N1 plane lies ca. 1.0 Å below the S3′–S4′–N4′–C2–N3′ plane, the dihedral angle between the two being 17.5°. The dimer units are linked through long (3.435 Å) S1---S3″ contacts. The S3–S4---S1---S3″–S4″ sequence so generated forms a nearly planar array of sulfur atoms.

The interannular S---S distance in $[(Me_2N)CN_2S_2]_2$ is similar to that found in **4** (2.988 (2) Å).[3a] These values, along with the (mean) S---S distances observed in the eclipsed structure (3.109 Å) in **3**[4] clearly represent very weak interactions. Indeed, ESR studies on the monomer/dimer equilibrium for **1b** (R = Ph) indicate an enthalpy of association of near zero.[3d] On this basis it seems reasonable to assume that the mean structural parameters within the dimers (Table I) provide a good representation of the monomer structures. In support of this conclusion electron diffraction analysis of **1b** (R = CF_3) in the gas phase has revealed structural features that are identical (within experimental error) to those seen in the dimer **4**.[3a]

The crystallographic structures described above for the radical **1b** (R = NMe_2) as its dimer and the cation **1a** (R = NMe_2) with an SbF_6^- counterion indicate relatively unperturbed ground-state radical or cation rings for comparison with theory. The interpretation of the experimental structural data in terms of the computational results is developed below.

Computational Studies on the Structures of 1a and 1b (R = NH_2, NMe_2). (i) Computed Geometries of the Ground ($^2A_2$) States of 1b (R = NH_2 and NMe_2). The structure of the radical **1b** (R = NH_2) was optimized at both the 3-21G* and 6-31G* UHF SCF levels. In general the calculated geometries (Figure 4a) obtained with the two basis sets are quite similar, bond lengths agreeing within 0.01–0.03 Å (the S–S distance) and angles within 1.5°. As might be anticipated from computational experience on smaller molecules[9] the larger 6-31G* set predicts shorter bond lengths (C–N = 1.330 vs 1.344 Å; S–N = 1.642 vs 1.647 Å; S–S = 2.083 vs 2.116 Å). Nonetheless, the general agreement between the 6-31G* and 3-21G* geometries provides confidence for the

(17) Møller, C.; Plesset, M. S. *Phys. Rev.* **1934**, *46*, 618.
(18) Krishnan, R.; Pople, J. A. *Int. J. Quantum Chem. Symp.* **1977**, *11*, 149.
(19) Höfs, H.-U.; Mews, R.; Clegg, W.; Noltemeyer, M.; Schmidt, M.; Sheldrick, G. M. *Chem. Ber.* **1983**, *116*, 416.

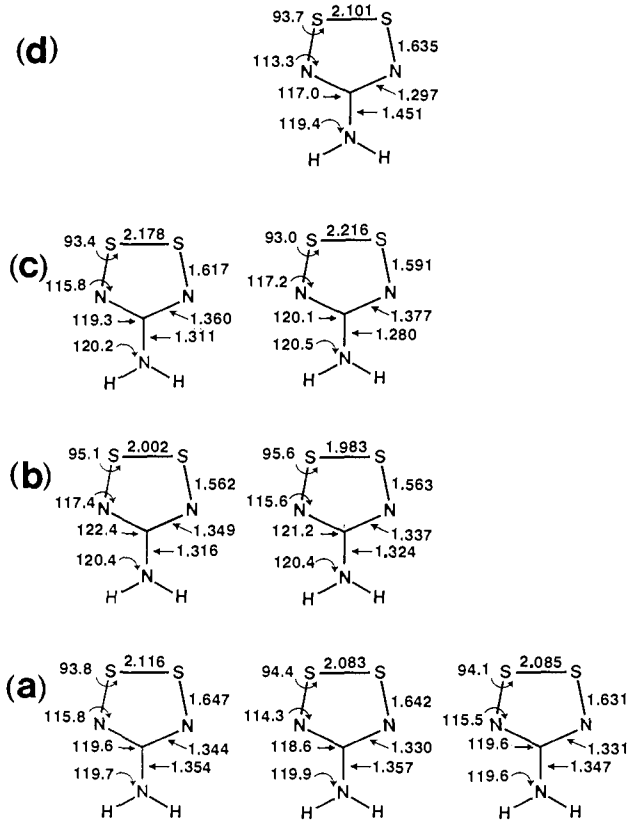

Figure 4. Optimized geometries at different levels of theory (from left to right) for the amino radical **1b** (R = NH_2) and the first three cationic states of **1a** (R = NH_2): (d) $^1B_2$, 3-21G* ROHF; (c) $^3B_2$, 3-21G* UHF, 3-21G* ROHF; (b) $^1A_1$, 3-21G* HF, 6-31G* HF; (a) $^2A_2$, 3-21G* UHF, 6-31G* UHF, 3-21G* ROHF.

somewhat smaller 3-21G* set used in nearly all the other geometry optimization calculations in this study.

With the same 3-21G* basis, both the UHF and ROHF geometries of the $^2A_2$ state of **1b** (R = NH_2) were determined (Figure 4a). Such a procedure was followed since at the UHF optimum geometry the value of $\langle S^2 \rangle$ was ca. 0.94 (ideal value 0.75), indicating the possibility of some spin contamination effects.[20] The UHF geometry showed a more delocalized structure with uniformly longer bonds while the ROHF bond lengths tend to alternate.[21] The ROHF predictions are probably to be preferred.

Both the differences in the 3-21G* UHF and ROHF geometries and the spin contamination effects found for **1b** (R = NMe_2; Figure 5) are highly reminiscent of those discussed above for **1b** (R = NH_2). Moreover the endocyclic bonds in both species (at both the UHF and ROHF levels) differ by less than 0.004 Å; the angles agree within 0.6°. The replacement of two protons by two methyl groups clearly has no substantive effect upon geometries. Although such a structural result is usually presumed in many computations where an NMe_2 substituent is replaced by an NH_2 group, its direct demonstration in this instance is gratifying.

Comparison of the five unique heavy-atom bond lengths in the crystal structure of the dimer $[(Me_2N)CN_2S_2]_2$ with the 3-21G* ROHF calculated values for free radical **1b** (R = NMe_2; Figure 5a) shows very good agreement; the average absolute deviation is only 0.009 Å, the largest difference 0.018 Å. Most notably, the calculation reproduces the S–S (2.082 Å calcd, 2.080 Å exptl) and S–N (1.627 Å calcd, 1.627 Å exptl) distances and the SSN angles (94.01° calcd, 95.0° exptl) extremely well. This agreement is further evidence for the very weak interactions involved in the radical dimer with the long interannular S---S contact and lends some credence to the predicted structure (Figure 4a) of the unobserved 4-amino radical.

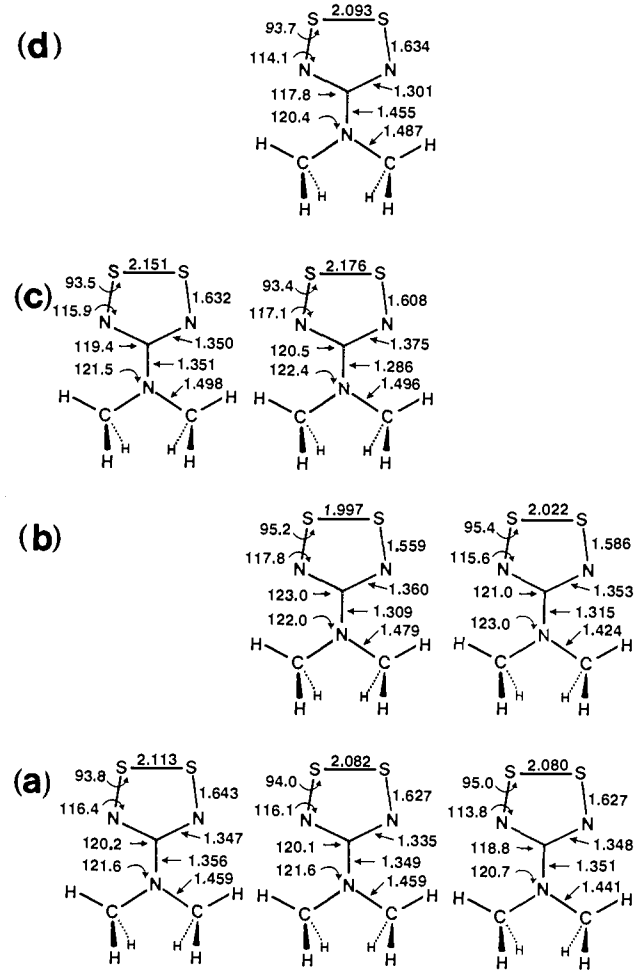

Figure 5. Optimized geometries at different levels of theory and experiment (from left to right) for the dimethylamino-substituted radical **1b** (R = NMe_2) and the first three cationic states of **1a** (R = NMe_2): (d) $^1B_2$, 3-21G* ROHF; (c) $^3B_2$, 3-21G* UHF, 3-21G* ROHF; (b) $^1A_1$, 3-21G* HF, crystal structure (mean); (a) $^2A_2$, 3-21G* UHF, 3-21G* ROHF, crystal structure (mean).

(ii) Computed Geometries of the Ground ($^1A_1$) States of 1a (R = NH_2, NMe_2). Figures 4b and 5b also present the optimized geometries for the closed-shell $^1A_1$ cations. As in the case of **1a** (R = NH_2) the effect of basis set expansion was tested by comparison of the 3-21G* and 6-31G* geometries. The effect is small, the largest change being in the S–S distance, which decreases from 2.002 Å (3-21G*) to 1.983 Å (6-31G*), i.e., a 1% contraction.

The structural changes that accompany ionization of the 3-21G* ROHF $^2A_2$ radicals **1b** (R = NH_2, NMe_2) to the 3-21G* HF cations **1a** (R = NH_2, NMe_2), which is of relevance to the UPS work (below), can all be related to the bonding/antibonding properties of the a_2 singly occupied molecular orbital (SOMO; Figure 1). Accordingly, the S–S and S–N distances of both radicals are significantly shortened upon ionization (see Figures 4 and 5 and Table I). To a first approximation the removal of an electron from the a_2 SOMO should not affect the endocyclic or exocyclic C–N distances (the carbon atom lies along a nodal plane). Ionization of **1b** (R = NH_2) nonetheless produces a small increase in the endocyclic C–N distance and a correspondingly (to "saturate" the valence of carbon) small decrease in the exocyclic C–N distance. Similar changes are observed in the ionization of **1b** (R = NMe_2); the endocyclic C–N distance increases slightly, and the exocyclic C–N contact shortens, this despite the expected steric hindrance from the methyl groups.[22] In response

(20) Farnell, L.; Pople, J. A.; Radom, L. *J. Phys. Chem.* **1983**, *87*, 79.
(21) This tendency for UHF methods to generate bond lengths of intermediate length, while ROHF bond distances tend to alternate, can be seen in the CH_2CN radical. See: Delbecq, F. *Chem. Phys. Lett.* **1983**, *99*, 21.
(22) Bondi, A. *J. Phys. Chem.* **1964**, *68*, 441.

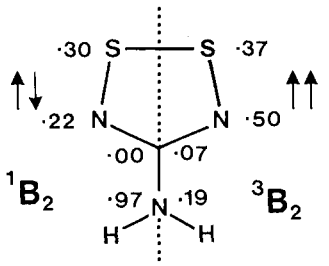

Figure 6. 3-21G* ROHF atomic spin populations for the $^1B_2$ (left) and $^3B_2$ (right) excited states of the 4-amino-1,2,3,5-dithiadiazolium cation **1b** (R = NH_2).

to this shortening in the exocyclic C–N bond, the N–CH_3 distances increase (from 1.459 Å in **1b** to 1.479 Å in **1a**).

The comparison of the computed and observed (X-ray) structural parameters of **1a** (R = NMe_2; Figure 5b) again shows an entirely satisfactory agreement between experiment and theory. Much of the difference may be due to the disorder in the crystal and consequent refinement problems. The average absolute deviation of ring bond lengths between theory and experiment is 0.016 Å, the largest discrepancy 0.027 Å. Most notably the calculation verifies the rather short exocyclic C–N bond (1.309 Å calcd, 1.315 Å exptl). The results are also entirely in keeping with the structural parameters for **1a** (R = Cl, CF_3; Table I).

(iii) Computed Geometries of the Excited ($^{1,3}B_2$) States of 1a (R = NH_2, NMe_2). The success of the calculations described above in replicating the observed experimental geometries for both the cation and radical systems provides a compelling argument for using similar level calculations to predict the geometries and energetics of the excited triplet ($^3B_2$) and open-shell singlet ($^1B_2$) states observed for $[(NMe_2)CN_2S_2]^+$ in the photoelectron and UV/vis spectra. In view of the generally unreliable performance of the UHF method for open-shell singlets,[23] only the ROHF method was used for the $^1B_2$ state. For the $^3B_2$ state both the UHF and ROHF 3-21G* geometries were calculated. At the final optimized UHF geometry, however, the value of $\langle S^2 \rangle$ was 2.147 (R = NH_2) and 2.208 (R = NMe_2; ideal value = 2.000), and this spin contamination suggests a somewhat greater reliability for the $^3B_2$ ROHF geometries.

Any orbital rationalization of the geometries of the excited states ($^3B_2$ or $^1B_2$) relative to that of $^1A_1$ must recognize the transfer of one electron from the b_1 HOMO of the ground-state cation to the more localized a_2 LUMO with the same (triplet) or opposite (open-shell singlet) spin as the remaining b_1 electron. Consistently with the phase properties illustrated in Figure 1, excitation of the $^1A_1$ cations to the corresponding $^3B_2$ cations induces a lengthening in the S–S, S–N, and endocyclic C–N distances and a contraction of the exocyclic C–N distance (Figures 4 and 5). In response to the contraction of the latter bonds, the N–CH_3 bonds lengthen slightly in order to offset any potential ring-methyl crowding.

The geometry of the $^1B_2$ open-shell singlet is most naturally compared with that of the $^3B_2$ triplet, which has the same orbital configuration. Interestingly the optimized geometries for **1b** (R = NH_2, NMe_2) differ markedly in these two states; the S–N bonds are longer in the singlet, while the endocyclic C–N bonds are shorter. The most dramatic changes, however, are in the exocyclic C–N bonds, which lengthen by over 0.17 Å, or 15%. As similar molecular orbitals are occupied in both these states, a purely one-electron argument cannot be used to account for such a large geometry difference. Some rationalization can be developed in terms of a many (two) electron model that considers electron repulsion. Analysis of the spin distributions (Figure 6) indicates very different electronic structures for the $^3B_2$ and $^1B_2$ states. For the triplet two electrons are concentrated within the ring, avoiding one another due to a Fermi hole. The open-shell singlet has two electrons of opposite spin and favors a situation in which one of the two electrons is essentially restricted to the ring (in the a_2 orbital), while the other is heavily localized on the exocyclic nitrogen (in the b_1 orbital).[24] Lengthening of the exocyclic C–N distance diminishes repulsion between these two singlet coupled electrons.

(23) Luke, B. T.; Pople, J. A.; Schleyer, P. v. R. *Chem. Phys. Lett.* **1983**, *97*, 265.

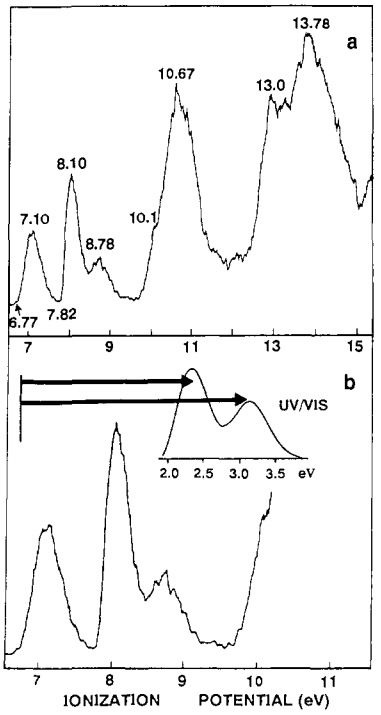

Figure 7. (a) He(I) photoelectron spectrum of the 4-(dimethylamino)-1,2,3,5-dithiadiazolyl radical (**1b**, R = NMe_2), and (b) the low-energy region of the photoelectron spectrum with the UV/vis spectrum (insert) of the cation **1a** (R = NMe_2).

Ultraviolet Photoelectron Spectrum of 1b, Ultraviolet/Visible Spectrum of 1a (R = NMe_2), and Computed Energies of Associated States. (i) **Photoelectron Spectrum.** The UPS of this radical (Figure 7, which also shows the values for the experimental IPs) is similar to those investigated previously,[5] in that ionization from the SOMO is separated from a cluster of ring IPs around 10–12 eV, followed by, in the case of the CF_3, Cl, and Ph analogues, many other IPs attributable to deeper lying ligand and ring orbitals. The unique feature of this spectrum is that the highest occupied orbital associated with the NMe_2 ligand, viz., Np π (b_1) (Figure 1), manifests itself as two distinct bands (IP_2, IP_3) around 8.5 eV in the approximate[25] intensity 3:1, which correspond to the first triplet and singlet excited states of the cation ($^{3,1}B_2$). This singlet/triplet splitting was not observed in the other spectra,[5] where the IPs were more nearly coincident. Although the focus of the present work is on these first three cationic states, we will, before considering these features in detail, summarize the assignment of the PE spectrum up to 15 eV in the context of the other radicals.

The other distinct feature of this spectrum is that the next four highest lying doubly occupied ring MOs, a_1, a_2, b_1, and b_2, all have IPs in a group at 10–12 eV, which comprises four triplet and four singlet states, although these have not been computed in this work. It is conceivable that some weak peaks attributable to singlet states occur around 12 eV, although it is anticipated that the exchange splitting is small for such delocalized orbitals. The intense band above 12 eV arises from further ring σ (a_1) and π (b_1) orbitals, which have been identified in the chloro derivative at 13.4 and 15.4 eV, respectively. Also occurring in this higher energy region will be bands arising from the methyl group π orbitals.[26]

(24) In effect the admixture of ligand and ring components in the b_1 orbital changes between the excited singlet and triplet cation states. In the singlet the b_1 orbital is heavily localized on the exocyclic nitrogen so as to reduce electron repulsion.

(25) Given the differences in the spin distributions noted earlier, some deviation from the 3:1 intensity ratio predicted from the spin multiplicities is to be expected.

Table II. Computed Total Energies (au) and Vertical and Adiabatic Ionization Energies (eV) for Amino-1,2,3,5-dithiadiazolyl Radical (**1b**, R = NH_2)

	vertical	adiabatic	vertical	adiabatic
	3-21G* UHF//3-21G* UHF			
$^3B_2$ cation	−992.243 14	−992.246 95	7.70	7.63
$^1A_1$ cation	−992.231 19	−992.247 79	7.98	7.61
$^2A_2$ radical	−992.527 45	−992.527 45	0.00	0.00
	3-21G* ROHF//3-21G* ROHF			
$^3B_2$ cation	−992.215 11	−992.226 34	7.98	7.67
$^1A_1$ cation	−992.236 14	−992.247 79	7.40	7.09
$^2A_2$ radical	−992.508 22	−992.508 22	0.00	0.00
	6-31G* UHF//3-21G* UHF			
$^3B_2$ cation	−997.061 33	−997.065 15	7.74	7.59
$^1A_1$ cation	−997.050 79	−998.067 75	8.06	7.52
$^2A_2$ radical	−997.344 11	−997.344 11	0.00	0.00
	6-31G* ROHF//3-21G* ROHF			
$^3B_2$ cation	−997.035 96	−997.043 58	7.95	7.74
$^1A_1$ cation	−997.050 79	−997.067 75	7.37	7.08
$^3A_2$ radical	−997.327 93	−997.327 93	0.00	0.00

Table III. Computed Total Energies (au) and Vertical and Adiabatic Ionization Energies (eV) for (Dimethylamino)-1,2,3,5-dithiadiazolyl Radical (**1b**, R = NMe_2)

	vertical	adiabatic	vertical	adiabatic
	3-21G* UHF//3-21G* UHF			
$^3B_2$ cation	−1069.910 09	−1069.913 23	6.60	6.52
$^1A_1$ cation	−1069.863 48	−1069.881 42	7.87	7.38
$^2A_2$ radical	−1070.152 80	−1070.152 80	0.00	0.00
	3-21G* ROHF//3-21G* ROHF			
$^3B_2$ cation	−1069.875 73	−1069.879 70	7.03	6.92
$^1A_1$ cation	−1069.868 35	−1069.881 42	7.23	6.87
$^2A_2$ radical	−1070.134 05	−1070.134 05	0.00	0.00
	6-31G* UHF//3-21G* UHF			
$^3B_2$ cation	−1075.154 79	−1075.156 54	6.62	6.47
$^1A_1$ cation	−1075.112 51	−1075.129 99	7.77	7.29
$^2A_2$ radical	−1075.398 03	−1075.398 03	0.00	0.00
	6-31G* UHF//3-21G* UHF			
$^3B_2$ cation	−1075.120 17	−1075.122 67	7.13	7.06
$^1A_1$ cation	−1075.118 70	−1075.129 99	7.17	6.87
$^2A_2$ radical	−1075.382 27	−1075.382 27	0.00	0.00

Any discussion of the first three bands must consider the Franck–Condon envelopes and the associated structural changes upon ionization, which have been clearly established from the ab initio calculations (Figure 5). Since no vibrational structure is resolved on any of the bands, it is sufficient to remark that the profile of the first band (vertical IP = 7.10 eV) is consistent with the removal of an antibonding electron, and the concomitant decrease in the S–S and S–N bond lengths as discussed above. The second band (vertical IP = 8.10 eV), corresponding to ionization from an orbital with considerable $p\pi$ localization on N is sharper. As mentioned, the calculated structures of the $^3B_2$ and $^1B_2$ states are different, and this is supported by the band widths of the associated IPs (fwhm of IP_2 (0.28 eV) and IP_3 (0.48 eV)).

Given the planarity at nitrogen in this radical, this is one of the few known instances where nitrogen lone-pair ionization is purely p in character[27] and explains the sharpness and low value (8.27 eV, weighted average) for the IP. Although the electronegative nature of the heterocyclic ring will tend to raise the IP somewhat, this compares favorably with a predicted IP for planar $(CH_3)_3N$ of 7.7–7.9 eV.[28]

(ii) Experimental and Theoretical Ionization Potentials. The experimental results described above provide an opportunity to test a variety of quantum mechanical procedures for their ability to determine IPs for states involving closed and open-shell singlets and involving triplets.

Table IV. Computed Total Energies and Adiabatic Energy Differences for the $^3B_2$ and $^1B_2$ States of the Amino and Dimethylamino Cations **1a** (R = NH_2, NMe_2)

	$[(H_2N)CN_2S_2]^+$		$[(Me_2N)CN_2S_2]^+$	
	E, au	ΔE, eV	*E*, au	ΔE, eV
	3-21G* ROHF//3-21G* ROHF			
$^1B_2$ cation	−992.185 93	1.10	−1069.861 25	0.50
$^3B_2$ cation	−992.226 34	0.00	−1069.879 70	0.00
	6-31G* ROHF//3-21G* ROHF			
$^1B_2$ cation	−997.004 30	1.07	−1075.107 60	0.41
$^3B_2$ cation	−997.043 58	0.00	−1075.122 67	0.00

Tables II (R = NH_2) and III (R = NMe_2) collect the SCF total energies (atomic units) and the energy differences (electronvolts) for the vertical and adiabatic IPs from the $^2A_2$ radical to the $^1A_1$ cation and the $^3B_2$ excited-state cation. As discussed previously for the geometries, the parent amino species is included, since it provides one way of extrapolating electron correlation effects to the NMe_2 species. The choice of ROHF or UHF geometries, as well as 3-21G* versus 6-31G* basis sets was also considered. Table IV collects the ROHF results on the $^1B_2$ open-shell excited-state cations (R = NH_2, NMe_2).

For the $^1A_1$ and $^3B_2$ states the 6-31G* energy differences differ from the 3-21G* values by <0.1 eV in all cases for both species, at a particular geometry (UHF or ROHF); the 6-31G* values are preferred for the IPs. However, the choice of optimized geometry from the two wave functions can lead to energy differences of up to 0.6 eV, although as indicated in the discussion on structures, the ROHF geometries are favored.

4-Amino-1,2,3,5-dithiadiazolyl Radical (1b, R = NH_2). For the amino species the ΔSCF results (6-31G* ROHF//3-21G*, Table II) predict vertical and adiabatic IPs to the $^1A_1$ state (IP_1) of 7.37 and 7.08 eV, respectively. For the IPs to the $^3B_2$ state (IP_2) the corresponding vertical and adiabatic energies are 7.95 and 7.74 eV, respectively. This leads to a difference between the two relaxed (adiabatic) states of 0.66 eV. It should be remembered that these ΔSCF results, if they are to be compared with experiment (as in the NMe_2 case), must be extended to include correlation. The need for this correction is great since the $^1A_1$ state has one more electron pair (and more to gain when correlation is included) compared to the $^3B_2$ state.[29] The problem is less severe for the $^2A_2$ radical vs the $^1A_1$ cation, since they have the same number of electron pairs, differing only by a singly occupied orbital. Within the GAUSSIAN86 program[11] correlation is usually included via Møller–Plesset perturbation theory, with an UHF wave function. To maintain consistency, the correlation correction calculations were carried out on the amino radical and cation at UHF optimized geometries.

The results of the Møller–Plesset treatment of correlation, starting from an UHF wave function, are shown in Table V for the larger 6-31G* basis set. The results of second-, third-, and partial fourth-order perturbation show a decrease for the $^1A_1$ ion and an increase for the $^3B_2$ cation. The (U)MP2 values overestimate the differential electron correlation effects between the two states, while the more reliable (U)MP3 and (U)MP4SDQ methods give values close to each other. For the amino species the best vertical IPs are then 6.86 ($^1A_1$) and 8.33 eV ($^3B_2$); the adiabatic values show analogous behavior, 6.77 ($^1A_1$) and 8.07 eV ($^3B_2$), giving a cation singlet–triplet excitation of 1.3 eV.

The remaining $^1B_2$ state is predicted, at the ROHF level (Table IV), to lie some 1.07 eV (adiabatic) above the triplet. In view of the fact that these states involve the same number of doubly occupied MOs, inclusion of correlation is unlikely to change this result significantly.

4-(Dimethylamino)-1,2,3,5-dithiadiazolyl Radical (1b, R = NMe_2). The SCF results for the states of this species, of relevance to the photoelectron spectrum are collected in Tables III and IV;

(26) Kimura, K.; Osafune, K. *Mol. Phys.* **1975**, *29*, 1073.
(27) An example of a very localized Np orbital in a planar environment is provided by manxine, with a coincident vertical/adiabatic IP of 7.05 eV. Aue, D. H.; Webb, H. M.; Bowers, M. T. *J. Am. Chem. Soc.* **1975**, *97*, 4136.
(28) Livant, P.; McKee, M. L.; Worley, S. D. *Inorg. Chem.* **1983**, *22*, 895.
(29) See, for example, the singlet–triplet splitting in methylene: Schaefer, H. F., III *Science* **1986**, *231*, 1100.

Table V. Effects of the Inclusion of Electron Correlation on the Total Energy (E) and the Vertical and Adiabatic Energy Differences (ΔE) for Amino-1,2,3,5-dithiadiazolyl Radical (**1b**, R = NH_2)[a]

	$^2A_2$	$^1A_1$		$^3B_2$	
	E, au	E, au	ΔE, eV	E, au	ΔE, eV
		Vertical			
(U)HF	−997.344 11	−997.050 79	7.98	−997.061 33	7.70
(U)MP2	−998.178 02	−997.960 06	5.93	−997.863 71	8.55
(U)MP3	−998.204 33	−997.954 58	6.80	−997.896 70	8.37
(U)MP4SDQ	−998.219 97	−997.967 72	6.86	−997.913 86	8.33
		Adiabatic			
(U)HF	−997.344 11	−997.067 75	7.52	−997.065 15	7.59
(U)MP2	−998.178 02	−997.959 32	5.95	−997.876 29	8.21
(U)MP3	−998.204 43	−997.958 75	6.69	−997.907 12	8.09
(U)MP4SDQ	−998.219 97	−997.971 16	6.77	−997.923 47	8.07

[a] All computations employed the 6-31G* basis set and the UHF method for the open-shell species and were performed at 3-21G* UHF optimized geometries.

Table VI. Effects of the Inclusion of Electron Correlation on the Total Energy (E) and the Vertical and Adiabatic Energy Differences (ΔE) for (Dimethylamino)-1,2,3,5-dithiadiazolyl Radical (**1b**, R = Me_2N)[a]

	$^2A_2$	$^1A_1$		$^3B_2$	
	E, au	E, au	ΔE, eV	E, au	ΔE, eV
		Vertical			
(U)HF	−1070.152 80	−1069.863 48	7.87	−1069.910 09	6.60
(U)MP2	−1070.965 19	−1070.760 81	5.56	−1070.693 16	7.40
(U)MP3	−1070.999 90	−1070.760 70	6.51	−1070.735 16	7.20
(U)MP4SDQ	−1071.026 83	−1070.790 45	6.43	−1070.762 27	7.20
		Adiabatic			
(U)HF	−1070.152 80	−1069.881 42	7.38	−1069.913 23	6.52
(U)MP2	−1070.965 19	−1070.759 20	5.61	−1070.697 86	7.27
(U)MP3	−1070.999 90	−1070.765 03	6.39	−1070.739 48	7.09
(U)MP4SDQ	−1071.026 83	−1070.793 41	6.35	−1070.766 81	7.08

[a] All computations employed the 3-21G* basis set and the UHF method for open-shell and were performed at 3-21G* UHF optimized geometries.

Møller–Plesset results are given in Table VI. The comments expressed above are equally relevant here but, in addition, it should also be noted that due to computational limitations correlation calculations were not explicitly performed for this species with the largest 6-31G* basis set. Instead correlation corrections were approached in two ways, viz., by extrapolation from the 6-31G* MP results for the smaller amino species or from smaller basis 3-21G* MP data obtained on the larger dimethylamino derivative, which were then applied to the 6-31G* results.

At the SCF level the vertical IP (6-31G* ROHF//3-21G*) to the $^1A_1$ cation (IP_1) is calculated to be 7.17 eV, which compares remarkably well with the experimental value of 7.10 eV. The calculated adiabatic value is 6.87 eV (experimental, 6.77 eV). For the $^3B_2$ state (IP_2) the ΔSCF values of 7.13 (vertical) and 7.06 eV (adiabatic) clearly require some correlation corrections which, as mentioned, are more appropriately added on to the UHF values.

The 6-31G* (U)MP4SDQ extrapolation from the amino species (Table V) requires a subtraction of 1.12 eV for the $^1A_1$ state and an addition of 0.63 eV for the $^3B_2$ state, giving vertical values of 6.65 eV for IP_1 (exptl 7.10 eV) and 7.25 for IP_2 (exptl 8.10 eV). This scheme directly applied to the dimethylamino species but with the smaller 3-21G* basis set (Table VI) yields corrections of −1.44 and +0.60 eV for the $^1A_1$ and $^3B_2$ ionization potentials (IP_1, IP_2). Applying these corrections to the 6-31G* UHF vertical ionizations of 7.77 eV for IP_1 and 6.62 eV for IP_2 (Table III) yields predicted values of 6.33 and 7.22 eV, respectively, with a separation of 0.89 eV.

Either correction scheme yields values for IP_1 and IP_2 too small relative to experiment, but the second performs better at assessing the difference between the two IPs, ca. 0.9 eV (calcd) compared to ca. 1.0 eV (exptl). From the ROHF results the $^1B_2$ open-shell singlet is computed to lie (adiabatically) 0.4 eV above the triplet. The corresponding experimental value can be estimated at 0.48 ± 0.1 eV (Figure 7).[30]

(30) A calculated ROHF vertical energy difference between the $^{1,3}B_2$ states was also determined (1.51 eV), but there is no experimental number for comparison.

(iii) UV/vis Spectrum and Excitation Energies. Since the photoelectron spectrum of a radical is essentially the UV/vis spectrum of the corresponding cation, a direct comparison of the UPS of **1b** (R = NMe_2) with the UV/vis spectrum of **1a** (R = NMe_2) is possible. Accordingly, the UV/vis spectrum of **1a**, with two bands at 2.33 and 3.12 eV (corresponding to the λ_{max} values of 532 and 398 nm, respectively), has been superimposed in register with the UPS in Figure 7b. A low-energy transition (at 533 nm) has also been observed in the R = NEt_2 derivative,[31] and the present results on the NMe_2 species clearly confirm that this is a $\pi-\pi^*$ transition from the energy difference (2.01 eV) between the $^1A_1$ adiabatic and $^1B_2$ vertical IPs.[32] The higher energy band is more difficult to assign; our calculated orbital energies suggest a variety of possible excitations at this approximate wavelength. A band at 388 nm was, in the NEt_2 work, ascribed to a $\sigma-\pi^*$ transition[31] (equivalent to the next Koopmans' IP above 10 eV) on the basis of HFS calculations. Figure 7b illustrates, however, that this second band (at 3.12 eV) partially overlaps the low-energy transition at 2.33 eV (532 nm) but falls short of the next IP. This lack of direct correspondence between the UV/vis and the UPS suggests that the UV/vis band may arise from a non-Koopmans' state involving a HOMO to (LUMO + 1) excitation not accessible by one-electron ionization. The absence of this excitation in the R = *t*-Bu, CCl_3, or Ph derivatives[31a] implies that it is a ligand-based process.

Summary and Conclusions

This work provides a clear view of the molecular structures of the ground states of the cation **1** and radical **2** (R = NMe_2), from both an experimental (X-ray diffraction) and theoretical (ab initio) point of view. The agreement is impressive and provides some

(31) (a) Chivers, T.; Edelmann, F.; Richardson, J. F.; Smith, N. R. M.; Treu, O.; Trsic, M. *Inorg. Chem.* **1986**, *25*, 2119. (b) Treu, O.; Trsic, M. *J. Mol. Struc. (THEOCHEM)* **1985**, *133*, 1.

(32) The discrepancy between these values arises from differences in the Franck–Condon factors associated with the ionization and absorption transitions. The former are evident from the calculated structures (Figure 5). Consequently, although we must take the adiabatic/vertical measurement, this is clearly only an approximation and can be regarded as a lower bound.

confidence in the predicted structural features for the hitherto unobserved 4-amino radical. Theory has also accurately specified the structures and energetics of the manifold of excited states of the cation **1a**, the former of considerable interest and often not available, and the latter for comparison with experiment, viz., photoexcitation (UV/vis) of **1a** or photoionization (UPS) of **1b**. To achieve accuracies beyond the simple Koopmans' theorem arguments and verify the assignment of the low-energy region of the photoelectron spectrum, electron correlation to partial fourth order was required.

Acknowledgment. The technical assistance of W.-T. Chan in performing the ROHF open-shell singlet calculations using GAMESS is acknowledged. Funding, in the form of operating grants, was provided by the Natural Sciences and Engineering Research Council of Canada (NSERC) (to J.D.G., R.T.O., and N.P.C.W.), the ESPCOR program of the National Science Foundation (to A.W.C.), and the State of Arkansas. Calculations on the Ontario Centre for Large Scale Computation CRAY-XMP/22 were made possible through a time allocation grant to J.D.G. under the NSERC Supercomputer Access Program.

Supplementary Material Available: Tables of crystallographic data (S1), atomic coordinates (S2), bond and angle data (S3 and S4), and anisotropic thermal parameters (S5) for $[(Me_2N)CN_2S_2]_2$ (S1) and $[(Me_2N)CN_2S_2]^+[SbF_6]^-$ (11 pages); tables of calculated and observed structure factors (31 pages). Ordering information is given on any current masthead page.

Effect of Electron Correlation on Atomic Electron Populations

John E. Carpenter, Mark P. McGrath, and Warren J. Hehre*

Contribution from the Department of Chemistry, University of California, Irvine, California 92717. *Received January 3, 1989*

Abstract: Atomic electron populations for a variety of molecules have been calculated at the HF/6-31G* and MP2/6-31G* levels using the natural population analysis method of Weinhold and co-workers. Correlation effects on electron populations act consistently to reduce charge separation and may be interpreted in terms of redistribution of electron density from high-lying filled molecular orbitals into low-lying unfilled orbitals.

Electron correlation is known to have significant influence on the properties of molecular systems. Extensive systematic studies of electron correlation effects as estimated from Møller–Plesset (MP) and configuration interaction (CI) models on equilibrium geometries[1,2] and normal-mode vibrational frequencies[2,3] have been reported. Bonds between electronegative elements were found to lengthen significantly, with a corresponding decrease in harmonic stretching frequencies. The role of electron correlation in altering relative thermochemical stabilities has also been examined.[2] Correlated descriptions generally appear to favor unsaturated and hypervalent bonding arrangements as opposed to the Hartree–Fock model, which tends to favor more conventional bonding patterns. Systematic investigations of correlation effects on atomic charge distributions have not previously been carried out and are the subject of the present report.

Quantum Mechanical Methods

All calculations have been carried out using the second-order Møller–Plesset (MP2) model for treatment of electron correlation[4,5] and the 6-31G* basis set.[6] Unless otherwise noted, all geometries correspond to HF/6-31G* optimized values. The SPARTAN system of electronic structure programs[7] has been employed.

The assessment of correlation effects on atomic electron populations is based on the natural population analysis of Weinhold and co-workers,[8] although reference has also been made to the more commonly-employed Mulliken scheme.[9]

Results and Discussion

Calculated atomic charges for formaldehyde obtained from Hartree–Fock and MP2 densities

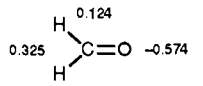

RHF/6-31G*

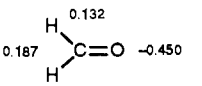

MP2/6-31G*

exhibit differences that are typical of many systems examined to date. Differences in HF and MP2 atomic charges appear to be relatively insensitive to basis set. For example, HF and MP2 charges, as well as differences between the two sets of charges for formaldehyde obtained at the 6-31+G* level

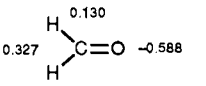

RHF/6-31+G*

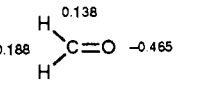

MP2/6-31+G*

are nearly identical with those obtained at the 6-31G* level (above). Correlation corrections of similar magnitude are also

(1) (a) DeFrees, D. J.; Levi, B. A.; Pollack, S. K.; Hehre, W. J.; Binkley, J. S.; Pople, J. A. *J. Am. Chem. Soc.* **1979**, *101*, 4085–4089. (b) DeFrees, D. J.; Krishnan, R.; Schlegel, H. B.; Pople, J. A. *J. Am. Chem. Soc.* **1982**, *104*, 5576–5580.

(2) For a general discussion, see: Hehre, W. J.; Radom, L.; Schleyer, P. v. R.; Pople, J. A. *Ab Initio Molecular Orbital Theory*; Wiley: New York, 1986.

(3) Hout, R. F., Jr.; Levi, B. A.; Hehre, W. J. *J. Comput. Chem.* **1982**, *3*, 234–250.

(4) (a) Møller, C.; Plesset, M. S. *Phys. Rev.* **1934**, *46*, 618–622. (b) Pople, J. A.; Seeger, R. *J. Chem. Phys.* **1975**, *62*, 4566.

(5) The frozen-core (valence-only) approximation has been employed. Calculations using this approximation yield atomic charges that are within +0.002 e of those obtained from all-electron calculations.

(6) (a) Hariharan, P. C.; Pople, J. A. *Theor. Chim. Acta* **1973**, *28*, 213–222. (b) Francl, M. M.; Pietro, W. J.; Hehre, W. J.; Binkley, J. S.; Gordon, M. S.; DeFrees, D. J.; Pople, J. A. *J. Chem. Phys.* **1982**, *77*, 3654–3665.

(7) Carpenter, J. E.; Hehre, W. J.; Kahn, S. D.; Weinhold, F. SPARTAN, a system of molecular electronic structure programs for large-memory, vector-architecture computers, to be submitted for publication.

(8) Reed, A. E.; Weinstock, R. B.; Weinhold, F. *J. Chem. Phys.* **1985**, *83*, 735–746.

(9) Mulliken, R. S. *J. Chem. Phys.* **1955**, *23*, 1833–1840, 1841–1846, 2338–2342, 2343–2356.

0002-7863/89/1511-6154$01.50/0